

# Soil Pollution Source Identification in Southern Iran Using Geochemical Data as a Global Study Model

S. Abbasi<sup>b</sup>, H. Amanipoor<sup>b</sup>, S. Battaleb-Looie<sup>b</sup>, S. Pourmorad<sup>a,\*</sup>, and J. Darvishi Khatoni<sup>c</sup>

Received September 28, 2023; revised October 25, 2023; accepted October 30, 2023

**Abstract**—Geochemical data and accurate statistics are critical in environmental studies to identify sources of soil contamination and reduce costs. A comprehensive understanding of investigation methods and data interpretation is a current challenge. This study presents innovative techniques for investigating soil contamination that can be applied worldwide. Using sediment samples from the southern region of Iran, we analysed 38 samples with X-ray fluorescence (XRF) and inductively coupled plasma mass spectrometry (ICP-MS). Statistical analysis, including descriptive statistics, Kolmogorov-Smirnov test (K-S), correlation coefficients, cluster and factor analyses, was performed using SPSS software. Cluster analysis revealed two primary element sources: lithogenic and anthropogenic, likely from the Karun River, the Gachsaran Formation, and contamination from nearby oil platforms. The pollution indices showed moderate pollution values for Mg, Sr, Cr, Ni, Pr, and Cd. Geochemical indices RI, PLI, Igeo, EF, Cf, and NIPI assessed the extent of pollution. Integration of sedimentary and geochemical data identified the source of sand particles as reworked Neogene deposits and silt from marl layers in upstream evaporites. These techniques have potential global applications.

**Keywords:** soil pollution, soil geochemistry, Southern Iran, environmental pollution, pollution statistical analysis

**DOI:** 10.1134/S1028334X23602559

## INTRODUCTION

In recent decades, the relationship between environmental quality and geochemistry (the chemical composition of the Earth) has received considerable attention from researchers and experts. However, there are still numerous problems regarding the accuracy of such studies [6]. With the advancement of more precise study methods and the increase of accuracy, not only can the origin, transport, and other ancient characteristics of sediments and various rocks be determined, but also the state of environmental pollution in the study area can be evaluated with much higher precision [14]. Quaternary sediments are among the environments where various pollutants are abundant. These contaminants have both natural and anthropogenic origins, and the need to study them closely has always been recognized [20]. Man-made pollutants that play a major role in environmental pol-

lution include agricultural pollutants, petroleum residues, urban and rural runoff, industrial pollutants, and other pollutants that result directly from human activities [8]. Heavy metals are of particular concern because of their diversity and widespread distribution, stability and nondegradability, potential toxicity or deficiency, ability to enter the food chain, and biological and physiological effects in general [20]. Soils and sediments contaminated with heavy metals possess the potential to contaminate other environmental components such as water sources, air, and agricultural products, making their assessment crucial and vital [7]. In recent years, numerous studies have been conducted on the chemistry of sediments and pollutants to determine their degree of pollution. Most of these studies have focused on identifying human-induced factors. What distinguishes this research from other studies is the consideration of a crucial point: This study considers that sediment composition is strongly influenced by the geochemical and mineralogical parameters of the source rocks, resulting in a wide variety of geochemical compositions Love and Zumberge [8].

In this research, which is considered a model study for the study of soil pollution in other parts of the world, the chemical composition of surface sediments is investigated. First, a general understanding of the region is established through geological investigations to identify sources and learn about the general geolog-

<sup>a</sup> University of Coimbra, Centre of Studies in Geography and Spatial Planning (CEGOT), FLUC, Department of Geography and Tourism, Coimbra, Portugal

<sup>b</sup> Department of Geology, Khorramshahr University of Marine Science and Technology, Khorramshahr, Iran

<sup>c</sup> Department of Marine Sciences, Geological Organization of Iran, Tehran, Iran

\*e-mail: [omid2red@gmail.com](mailto:omid2red@gmail.com)

ical, tectonic, and mineralogical structure of the area. Then, geochemical data will be used to study the origin of the sediments and the distribution of various elements in the study area. Finally, by studying the geochemistry of heavy metals and their bioavailability, a better assessment of their environmental impact can be made. The importance of geochemical studies in the study area is emphasised by the fact that the study area includes several densely populated villages and is considered part of the active agricultural and ecological zones of Iran, making it a potentially ideal model for similar studies around the world. In addition, this study outlines the methodology for a detailed geochemical study of sediments and explains how these studies correlate with statistical data for conducting similar studies.

### GEOGRAPHICAL AND GEOLOGICAL LOCATION

The studied area is located in the south of Iran, in the Khuzestan province, and in the vicinity of the city of Gotvand. Overall, the geology of the study area in Khuzestan Province is characterized by a variety of landforms, including mountains, hills, plateaus, and plains, which have been formed over millions of years by tectonic forces, erosion, and depositional processes [4]. The geological formations of the Khuzestan area, which is part of the folded and thrust Zagros, were formed under different sedimentary and tectonic conditions; therefore, the differences in facies are important in terms of time and place [19]. Based on the factors of lithology, tectonics and age of the geological formations, the rock outcrops of the province can be divided into the following two tectonostratigraphic units [3]: A: marine sequences of Jurassic-Cretaceous age, which have facies of the young Tethys basin. The aforementioned series are generally exposed in the core of the anticlines and in a general northwest-southeast direction; B: Sequences associated with alpine orogeny, Cenozoic, and whose features represent deposits accumulated in a southward retreating sea. The sequence in question, which may be marine or non-marine, includes the following units [9]: first, marine series of Eocene age (Pabde Formation) and marine limestones of Oligocene and Miocene age (Asmari Formation), which form the reservoir rocks of the province's petroleum reserves. Second, the Miocene clastic evaporite units known as the Fars Group were formed at the same time as the end of the Alpine orogeny and in retreating marine environments. The evaporite series at the base of this complex (Gachsaran Formation) are the oil deposits of Khuzestan Province. Thirdly, the detrital units after the orogeny are known as Bakhtiari Conglomerate, which represents a relatively strong erosion after the end of the Alpine orogeny. Finally, there are the Quaternary debris deposits, which are the result of weathering of various formations [2]. Apart from the Khuzestan

plain, which is relatively quiet and has no seismic force, the seismic force is high in the mountainous regions of the province, especially around Behbahan, which is sometimes associated with damage and destruction [4]. Figure 1 shows the geologic location of the area studied the geologic map of the area studied along with the names and lithology of the various formations.

### RESEARCH METHODOLOGY

The research method and its implementation play a crucial role in the outcome of the data. In this study, which was conducted as a global model research, the following steps were performed sequentially:

—Office studies: these studies include all preliminary research conducted prior to fieldwork. The most important aspects of these studies include the collection and analysis of books, maps, and relevant articles, as well as the use of various aerial photographs of the study area (southwestern Iran—Gotvand Plain). The duration of these studies was over a period of four months.

—Preliminary field studies: this phase of the study includes various field investigations. Extensive knowledge of the geologic features of the area, including sedimentologic, tectonic, and mineralogic features, was acquired during this phase. The importance of these aspects to the transport and deposition of the various sediments was evaluated. A map of ideal sampling sites was then developed. These studies took place over a period of three months.

—Sampling: in this phase of the study, we collected 38 sediment samples containing silt, clay, and fine sand particles from different regions of the study area (Table 1). Our sampling strategy aimed to cover the entire study area, from near-mountainous areas to lowlands. At each sampling location, one kilogram of soil was collected manually with a hand auger at a depth of 20 centimeters below the surface. This depth was chosen to avoid surface contamination. After collection, samples were carefully labeled using sample bags. These labeled samples were then sent to the Central Laboratory of the Geological Survey of Iran for geochemical analysis. The analysis was performed using inductively coupled plasma mass spectrometry (ICP-MS) and X-ray fluorescence (XRF).

—Laboratory studies: This section of the study focuses on analysing and testing the results of the geochemical investigations. Data were processed and statistically analysed using SPSS software. This included evaluating the distribution of data through indices and statistical tests, performing correlation analyses, and identifying the sources of elements through cluster and factor analyses. SPSS (Statistical Package for the Social Sciences) is a software used for statistical analysis [5]. These experiments were conducted in the Central Laboratory of the Geological Organisation of

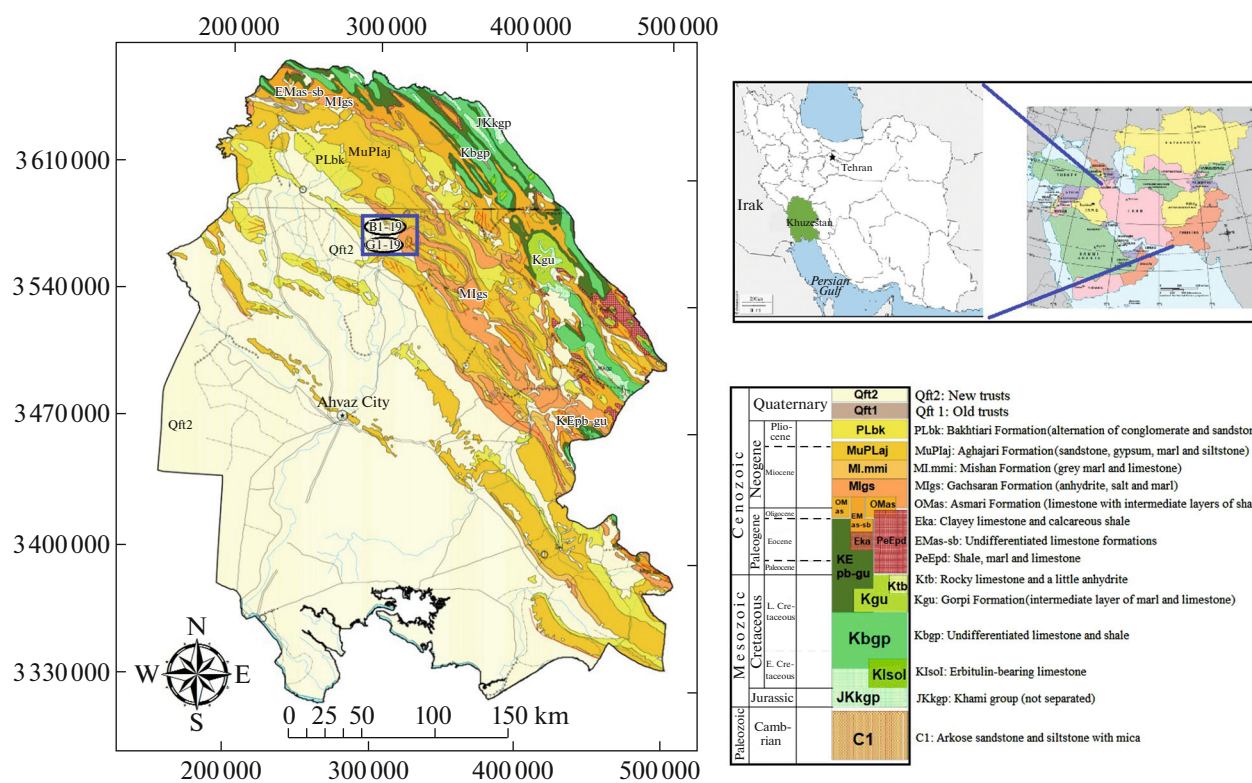


**Fig. 1.** Geographical and geological location of the study area along with the geographical location of the recorded samples (red circles).

Iran and in the Central Laboratory of the Department of Physical Geography of the University of Coimbra, Portugal.

## RESULTS AND DISCUSSION

### *Results of Geochemical Measurements*

One of the most effective methods in geochemical studies is the comparison of elemental composition between different sections in terms of the abundance of trace elements and oxides present in the samples [12]. Essentially, the abundance of various elements in each environment reflects the conditions of formation and the nature of the constituent environment, indicating the source of induced pollution [10]. Results obtained from the study of trace elements in the study area, considered as a global model, indicate that the most abundant trace element in the study areas is titanium (Ti). Following this element, the most abundant elements, in order, are strontium (Sr), phosphorus (P), and manganese (Mn) (Table 2). The results obtained from the study of oxides in the study area reveal that the most abundant oxides in the study area are, in order, calcium oxide (CaO) and silicon dioxide (SiO<sub>2</sub>). These data are based on the average percentage of oxides analysed in 31 samples of silts and clays (based on the predominant lithology) collected in the study area. The results obtained from the study

of oxides in the study area reveal that the most abundant oxides in the study area are, in order, calcium oxide (CaO) and silicon dioxide (SiO<sub>2</sub>) (Table 3 and Fig. 2). A comparison of oxide values in Fig. 3 demonstrates contrasting trends in SiO<sub>2</sub> and CaO variations in the study area, which could potentially be attributed to the presence of rock fragments within these sediments. Their presence might lead to an increase in the percentage of CaO and a relative decrease in SiO<sub>2</sub> [12]. It is suggested that if similar results are observed in other parts of the world, petrographic studies should be conducted to determine the percentage of rock fragments.

Particle size analysis of sediment samples can play a significant role in analyzing various data, especially in determining the sources of different contaminants in soil samples [20]. In this study, collected samples were categorized based on their probable sources into two groups: samples related to alluvial fans in the northern part of the area, originating from volcanic deposits (Late Miocene Bakhtiari Formation), and samples associated with alluvial fans in the eastern part of the area, likely originating from evaporite deposits (Early Miocene Gachsaran Formation).

The classification of different samples revealed that sedimentary and lithological samples in the northern part of the area are coarse-grained with weak rounding

**Table 1.** List of samples collected in the study area. These samples are labeled BK (for samples near the Bakhtiari Formation) and G (for samples near the Gachsaran Evaporative Formation)

Sample number	Lithology	The sampled quantity	Sample number	Lithology	The sampled quantity
BK1	Gravel, fine sand, and silt	2 kg	G1	Gravel, fine sand, and silt	2 kg
BK2	Gravel, fine sand, and silt	2 kg	G2	Gravel, fine sand, and silt	2 kg
BK3	Gravel, fine sand, and silt	2 kg	G3	Gravel, fine sand, and silt	2 kg
BK4	Silt, fine sand, and gravel	1 kg	G4	Silt, fine sand, and gravel	1 kg
BK5	Silt, fine sand, and gravel	1 kg	G5	Silt, fine sand, and gravel	1 kg
BK6	Silt, fine sand, and gravel	1 kg	G6	Silt, fine sand, and gravel	1 kg
BK7	Silt, fine sand, and gravel	1 kg	G7	Silt, fine sand, and gravel	1 kg
BK8	Silt, fine sand	1 kg	G8	Silt, fine sand	1 kg
BK9	Silt, fine sand	1 kg	G9	Silt, fine sand	1 kg
BK10	Silt, fine sand	1 kg	G10	Silt, fine sand	1 kg
BK11	Silt and clay	1 kg	G11	Silt and clay	1 kg
BK12	Silt and clay	1 kg	G12	Silt and clay	1 kg
BK13	Silt and clay	1 kg	G13	Silt and clay	1 kg
BK14	Silt and clay	1 kg	G14	Silt and clay	1 kg
BK15	Silt and clay	1 kg	G15	Silt and clay	1 kg
BK16	Silt and clay	1 kg	G16	Silt and clay	1 kg
BK17	Silt and clay	1 kg	G17	Silt and clay	1 kg
BK18	Silt and clay	1 kg	G18	Silt and clay	1 kg
BK19	Silt and clay	1 kg	G19	Silt and clay	1 kg

and poor sorting. Gradually, as distance increases from mountainous regions towards the plain, these samples transform from coarse to medium-sized particles and eventually to fine particles. The higher abundance of coarse-grained particles among finer-grained particles in the northern area indicates two important points. Firstly, the transporting floods carrying these sediments in the northern part of the area had higher velocity (not necessarily higher discharge), and secondly, the sediments were transported from environments with both humid and arid climates and under the dominance of physical degradation (Fig. 4). Samples from the eastern part, due to the high solubility of gypsum particles, initially appear as coarse-grained particles and eventually, after a distance of about one kilometer, completely transform into fine-grained particles.

In this study, for the geochemical and statistical analysis of elements, determining the relationship between major and trace elements, as well as achieving a specific genetic pattern, assessing the elemental contamination of the region, and identifying the sources of contamination in terms of their potential to generate dust, analyzing toxic and heavy element anomalies, and identifying the origins of elements in the plain, statistical analyses of major, trace, and rare elements

were conducted. In geochemical studies, various factors such as genetic factors can establish connections between variables. The degree of this dependence can be indicated by correlation coefficients [20]. In this method, by using regression and other statistical parameters, it is possible to identify the controlling factors and processes of sedimentation and to determine the role of natural and anthropogenic (man-made) factors in the distribution of sediments [13]. Before determining the correlation coefficient, one must first ensure the normality of the data distribution in order to use the appropriate coefficient based on that. As can be seen in Table 5, except Ba, Na, Sr, and Pr elements, other elements have a normal distribution. The distribution of these four elements was converted to normal using the logarithm method. Considering the normal distribution of elements in the sediment samples, the correlation between the study parameters was examined using the Pearson correlation coefficient. The results indicate a correlation among the investigated elements. The reason behind this is the lack of diversity in pollution sources in the study area (Table 6). In the cluster analysis based on the studied elements and sampling stations, an initial elimination of cases with low correlations was performed, leaving out elements that exhibited weak rela-

**Table 2.** Measurement results of different elements in the study area

Average in the upper crust	Domain	Minimum	Maximum	Standard deviation	Variance	Average	Parameter		No
8/40	3/4	1/50	4/44	5/50	5/5	2/4	wt %	Al	1
3/5	3	5/54	3/51	5/7	5/45	1/53		Fe	2
2/88	5/6	5/57	5/71	5/23	5/50	5/34		Na	3
2/8	5/4	5/31	1/54	5/21	5/50	5/62		K	4
1/33	1/6	5/00	2/14	5/42	5/14	1/64	ppm	Mg	0
0144	2475	662	3041	054.4	303246	1727		Ti	6
044	407	254	661	151/6	15324	450		P	7
044	144	34	146	116/4	13007	340		Mn	4
554	373	42	400	60/75	4325	164		Ba	5
354	1736	253	1535	417/7	17470	056		Sr	15
184	117	43/1	165	35/53	551/4	47/4		Zr	11
140	71	27/6	54/7	25/76	435/5	03/4		V	12
85	114	05	177	25/72	443/6	57		Cr	13
01	02	17/0	65/7	12/60	165/1	30/0		Zn	14
00	24	15	37/0	7/02	06/6	21/0		Ce	10
00	44	21	150	17/01	356/6	47/7		Ni	16
34	13	7/3	25/2	3/20	15/04	12/4		La	17
20	12	0/6	17/1	2/41	7/52	15/30		Nd	14
25	17	7/2	24/1	3/36	11/24	12/3		Cu	15
22	5/1	0/44	14/5	2/05	6/7	5/44		Y	25
10	14	0	14/5	3/41	11/62	5	Co	21	
13/0	4/2	2/47	15/7	2/25	0/20	0/63	Sc	22	
12	5/1	2/75	11/5	2/34	0/44	6/04	Nb	23	
14/0	3/3	1/30	4/64	5/52	5/44	2/62	Th	24	
0/1	10	1/60	16/4	2/65	7/20	3/02	Pr	20	
0/5	2/4	1/2	3/6	5/00	5/3	2/23	Sm	26	
3/8	2/1	1/56	3/10	5/44	5/23	2/51	Gd	27	
3/5	1/6	1/51	2/04	5/42	5/14	1/73	Dy	24	
2/3	1	5/01	1/46	5/20	5/56	1/51	Er	25	

**Table 3.** The results of measuring oxides by XRF device in terms of percentage

Oxide	TiO <sub>2</sub>	SrO	SO <sub>3</sub>	SiO <sub>2</sub>	P <sub>2</sub> O <sub>5</sub>	Na <sub>2</sub> O	MnO	MgO	K <sub>2</sub> O	Fe <sub>2</sub> O <sub>3</sub>	CaO	Al <sub>2</sub> O <sub>3</sub>	L.O.I
Minimum	5/56	/545	5/54	4/57	5/54	5/50	5/51	5/45	5/14	5/04	6/47	1/30	12/41
Maximum	5/67	/25 5	36/55	46/14	5/14	5/04	5/15	15/60	2/07	6/23	46/12	13/14	30/35
Mean	5/33	/105	6/71	24/43	5/12	5/23	5/50	4/35	1/12	2/54	24/50	6/33	24/61
Standard deviation	5/16	/56 5	5/35	5/25	5/53	5/13	5/52	2/70	5/65	1/44	11/74	3/44	6/17

tionships for subsequent analyses. Following the dendrogram resulting from the cluster analysis, post the exclusion of elements with minimal or absent correlations, which amounted to a total of 8 elements, the sampling stations were also categorized into two main groups based on the anomalies and element behaviors.

Specifically, sampling stations 4, 20, 5, 2, 1, 3, 7, 11, and 12 were grouped together, sharing common characteristics, potentially indicating exposure to similar anomalies or contaminations, or possibly originating from the same sedimentary environment. Furthermore, the second cluster reveals the presence of two

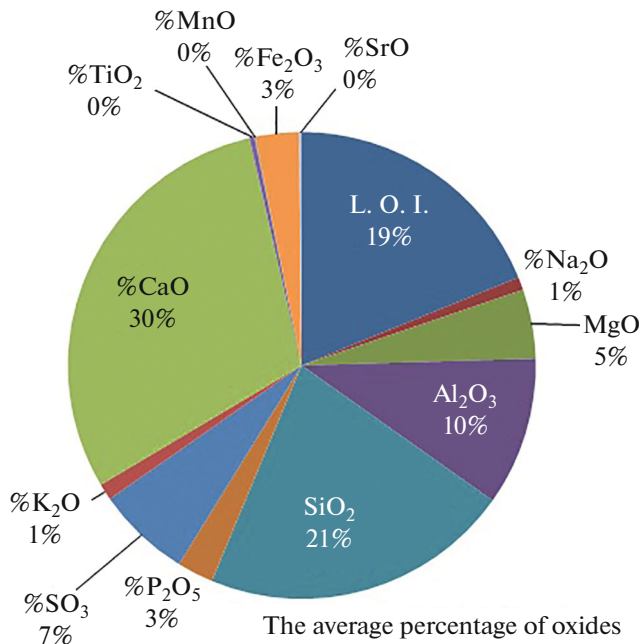


Fig. 2. The average percentage of oxides in the samples collected from the studied area.

subsets with high intercorrelations. The first subset encompasses stations 8, 10, 6, and 14, while the second subset involves stations 18, 22, 17, 19, 21, 15, 23, 16, 38, 27, 33, 31, 37, 13, and 25 (Figs. 5 and 6). In these figures, the numbers represent the identifiers of the sampling sites analyzed in this study, whose characteristics were examined and classified accordingly. Numbers 1 through 19 correspond to samples BK1 through BK19, and numbers 20 through 38 correspond to samples G1 through G19.

Based on these data, it is possible to infer the origin and genesis of each of the elements; such that elements exhibiting positive correlations are discernible by their

terrestrial origin. In the Dendrogram analysis, three main clusters can be identified. Elements Mn, Ni, Ce, Y, Al, Sm, K, La, and Dy form one cluster, elements V, Er, Zr, Co, and Mg form another cluster, and elements Ti, Th, Nd, and Gd form a subcluster within the third cluster. Additionally, elements Fe, Cr, Nb, Tl, Sc, and Ta form another subcluster within the third cluster. The determination of the number of clusters mentioned is based on the genetic behavior of the elements. It appears that clusters containing elements with established terrestrial origins, such as Fe, might signify a terrestrial source for those elements. The grouping of elements V, Er, Zr, Co, and Mg in one cluster, and Mn, Ni, Ce, Y, Al, Sm, K, La, and Dy in another, could potentially indicate a human-related origin for these elements; although the possibility of dual origins remains plausible in this context. Factor analysis involves three stages: data suitability assessment for analysis, factor extraction, and interpretation of results. The Kaiser-Meyer-Olkin (KMO) coefficient and Bartlett's Test of Sphericity are suitable tools to ensure the data's appropriateness for this analysis. Low KMO coefficient values (less than 0.5) indicate that the correlation between parameters cannot be explained by other parameters [5]. The KMO coefficient ranges between one and zero. If the KMO value falls between 0.5 and 0.69, cautious use of the analysis is possible, and if it exceeds 0.7, factor analysis can be employed for data decomposition and analysis [15]. The outcomes of this analysis are presented in Table 7, indicating the suitability of the data for factor analysis.

Based on factor analysis, elements with high correlation coefficients have been identified as a single factor. As depicted in Table 8 and Fig. 7, seven factors influence the distribution of elements in the study area, where approximately 50% of the variations are attributed to the first factor. The remaining six factors collectively contribute to less than 30% of the variations. According to this analysis, all measured

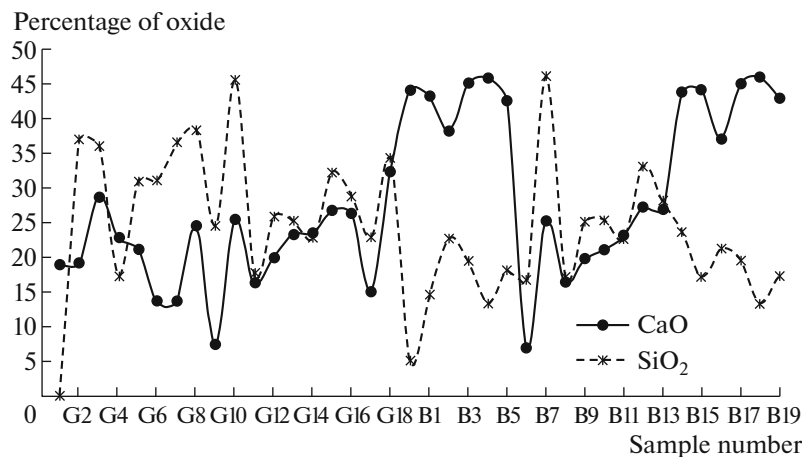


Fig. 3. Comparison of the changes of CaO versus SiO<sub>2</sub> in the studied area, which shows the reverse trend of these results.

**Table 4.** Granulation analysis results of some alluvial sediments

% Mud	% Sand	% Gravel	Y	X	No
<i>Granulation of sediments originating from Gachsaran Formatio (7 out of 19)</i>					
18/21	10/54	60/40	48°57'37.4"	32°11'43.2"	G1
35/08	11/16	03/50	48°57'21.2"	32°11'41.3"	G2
35/82	13/44	05/7	48°56'53.0"	32°11'44.7"	G3
58/00	11/1	25/44	48°56'31.7"	32°11'36.4"	G4
02/45	4/61	15/34	48°56'4.0"	32°11'31.5"	G5
08/08	7/7	13/41	48°55'38.7"	32°11'22.8"	G6
82/88	6/22	15/5	48°55'17.6"	32°11'16.2"	G7
<i>Granulation of sediments originating from Bakhtiari Formation (7 out of 19)</i>					
0/40	30/51	65/53	48°54'52.83"	32°13'40.65"	BK1
0/8	34/77	04/33	48°54'46.50"	32°13'32.76"	BK2
12/45	34/14	03/77	48°54'39.74"	32°13'28.54"	BK3
12/30	03/44	34/2	48°54'36.07"	32°13'21.94"	BK4
18/23	04/51	26/46	48°54'28.54"	32°13'15.39"	BK5
50/80	34/73	4/33	48°54'17.39"	32°13'7.88"	BK6
01/50	22/10	6/24	48°54'11.15"	32°12'55.98"	BK7

**Table 5.** The results of the K-S test on the studied sample

p-Value	Value	p-Value	Value	p-Value	Value
4/41	Nb	5/73	V	5/50	Al
4/48	Th	5/76	Cr	5/25	Fe
<b>4/44</b>	<b>Pr</b>	5/14	Zn	<b>5/551</b>	<b>Na</b>
4/24	Sm	5/25	Ce	5/51	K
4/24	Gd	5/25	Ni	5/52	Mg
4/13	Dy	5/17	La	5/25	Ti
4/24	Er	5/25	Nd	5/25	P
4/40	Ta	5/13	Cu	5/11	Mn
4/24	Tl	5/52	Y	<b>5/55</b>	<b>Ba</b>
4/24	Cd	5/15	Co	<b>5/55</b>	<b>Sr</b>
		5/53	Sc	5/25	Zr
Test results after normalization by logarithm method					
		p-Value	Value	p-Value	Value
		5/52	Sr	5/51	Na
		5/15	Pr	5/54	Ba

Significance level:  $\alpha/51$  <sup>1</sup>.**Table 6.** Results of correlation coefficients of studied elements The results of the K-S test on the studied sample

Ni	Zn	V	Sr	Ba	P	Mg	K	Na	Element
4/30	5/41		5/42	5/71 5/42	5/42		5/37	5/42	P Sr Cd
		-5/44				-5/34			



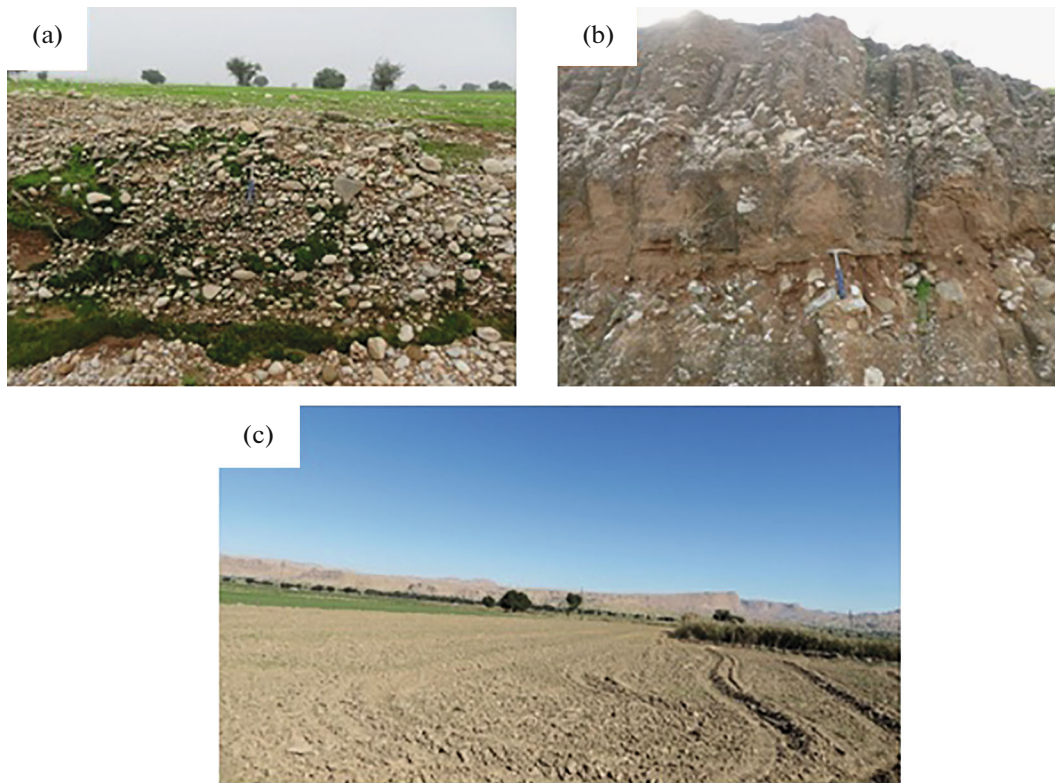


**Fig. 4.** Geological characteristics of the studied region. (a) The sedimentary facies and lithology in the upstream section originating from Bakhtiari formations in the northern part of the area. (b) Poor sedimentary facies and lithological variations in the upstream section sourced from Gachsaran formations in the eastern part of the area. (c) Distant outcrop from the downstream section in the eastern part of the area, facing southeast.

elements except Na and Pr have high factor loadings (above 0.5) in Factor 1 (Table 9). Considering the regional context, Factor 1 could potentially signify a terrestrial origin for elements present in sediments, likely derived from the erosion of various source rocks and transported into the basin through river systems [5].

The presence of various rivers, especially the Karun River, is a potential source for the mentioned elements. In Factor 2, elements Na and Mg exhibit the highest factor loadings. Evaporite minerals, particularly in the eastern part of the region (Gachsaran Formation), could potentially serve as the source for these elements. Elements Zr, V, and Er contribute the most to Factor 3's factor loadings. In Factor 4, elements Sc and Ta, in Factor 5, elements Pr and V,

and in Factors 6 and 7, respectively, Cr and V possess the highest factor loadings. Each of the Factors 2 to 7 indicates a distinct origin contributing to the creation of anomalies. It is conceivable that the presence of evaporites and upstream contaminations from various sources could lead to increased anomaly creation and the emergence of diverse factor loadings. The results of factor analysis further validate the findings of the cluster analysis.

Analysis of Environmental Indices Numerous environmental indices are available to assess pollution levels in soil samples. In this study, a variety of indices, including the Geoaccumulation Index, Enrichment Factor, Pollution Load Index, Ecological Risk Index, Pollution Load, and Contamination Degree, were employed for evaluating soil contamination levels. Various methods of studying environmental pollution using different indices yield fairly similar results for the studied samples. Studies conducted using the Geoaccumulation Index (Igeo) indicated that the investigated samples exhibited a status ranging from uncontaminated to moderately contaminated for most elements, except for elements such as Mg, Cr, Pr, Ni, Sr, and Cd, which were in the uncontaminated to moderately contaminated range. Based on the Enrichment Factor (EF) factor, the studied samples showed vary-

**Table 7.** KMO and Bartlett test results for the studied samples

KMO		4/58
Bartlett's of Sphericity	$\chi^2$	1344/37
	df	456
	Sig.	5/55



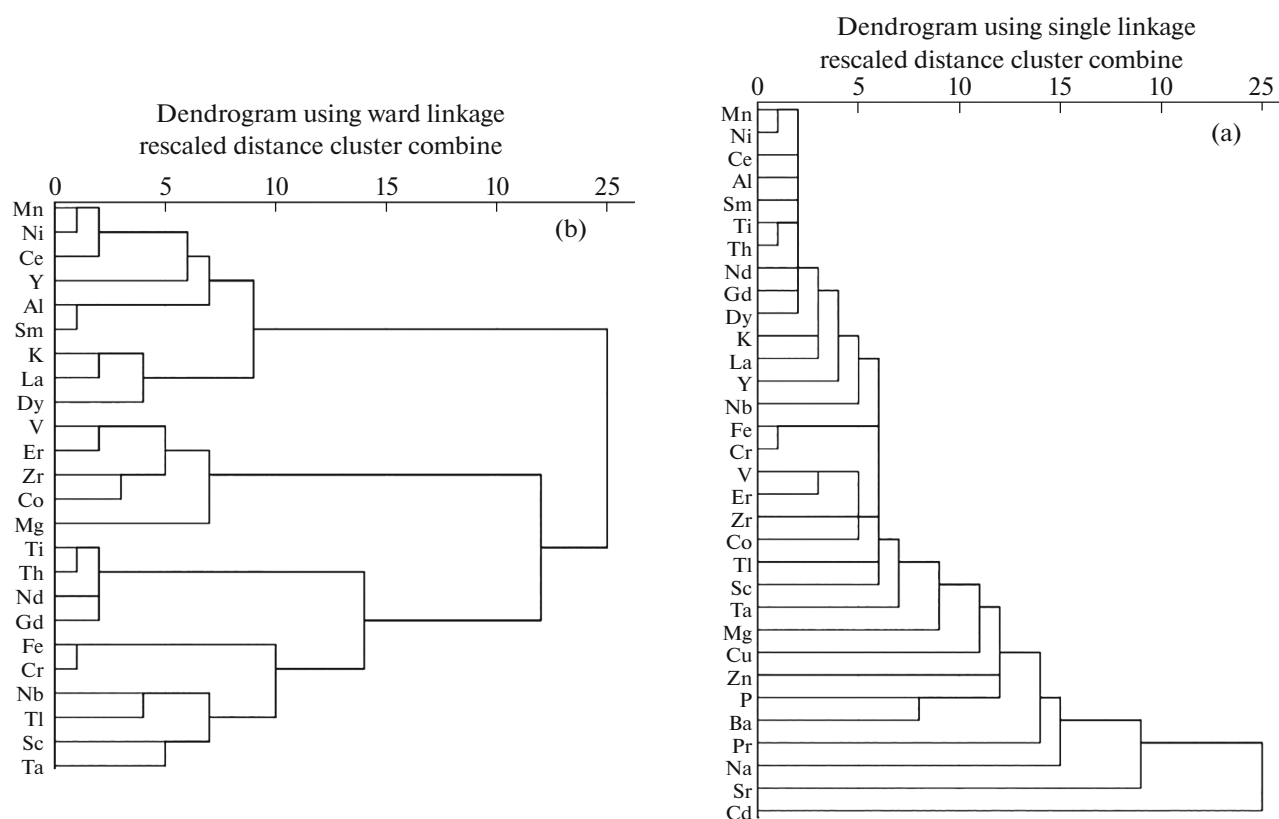


**Fig. 5.** Dendrogram resulting from cluster analysis for all studied elements: (a) before eliminating elements with low correlations, (b) after eliminating elements with low correlations.

ing percentages of enrichment levels from no enrichment to moderate enrichment for certain elements including Ti, P, Mn, V, Cr, Ni, Cu, Y, Co, Sc, Nb, Gd, Er, and Pr. Elements Sr, Mg, and Cd in some samples fell within the moderately enriched range. The investigation of Contamination Factors (CF) for the studied samples revealed that elements including Na, Mg, Mn, Cr, and Pr fall within the moderate range for

some samples. For elements Sr and Cd, certain samples exhibited values within a significant range. The assessment of pollution present in the area using the Nemerow Integrated Pollution Index (NIPI) indicated that these samples exhibit low pollution levels for elements like Mg, Cr, Ni, and Pr, while showing high pollution levels for elements Sr and Cd (Table 10). The examination of Modified Degree of Contamina-

**Table 8.** The table resulting from the total variance of the studied samples

Factor	Initial eigenvalues			Rounded values		
	special amount	variance explained	the cumulative percentage	special amount	variance explained	the cumulative percentage
1	14/17	44/46	44/63	13/57	44/15	44/15
2	2/54	7/52	00/44	1/45	6/25	04/34
3	1/77	6/12	62/55	1/60	0/75	65/54
0	1/04	0/31	67/31	1/04	0/33	60/41
5	1/35	4/74	72/15	1/45	0/14	75/00
0	1/23	4/20	76/34	1/47	0/57	70/62
0	1/50	3/62	75/56	1/26	4/34	75/56

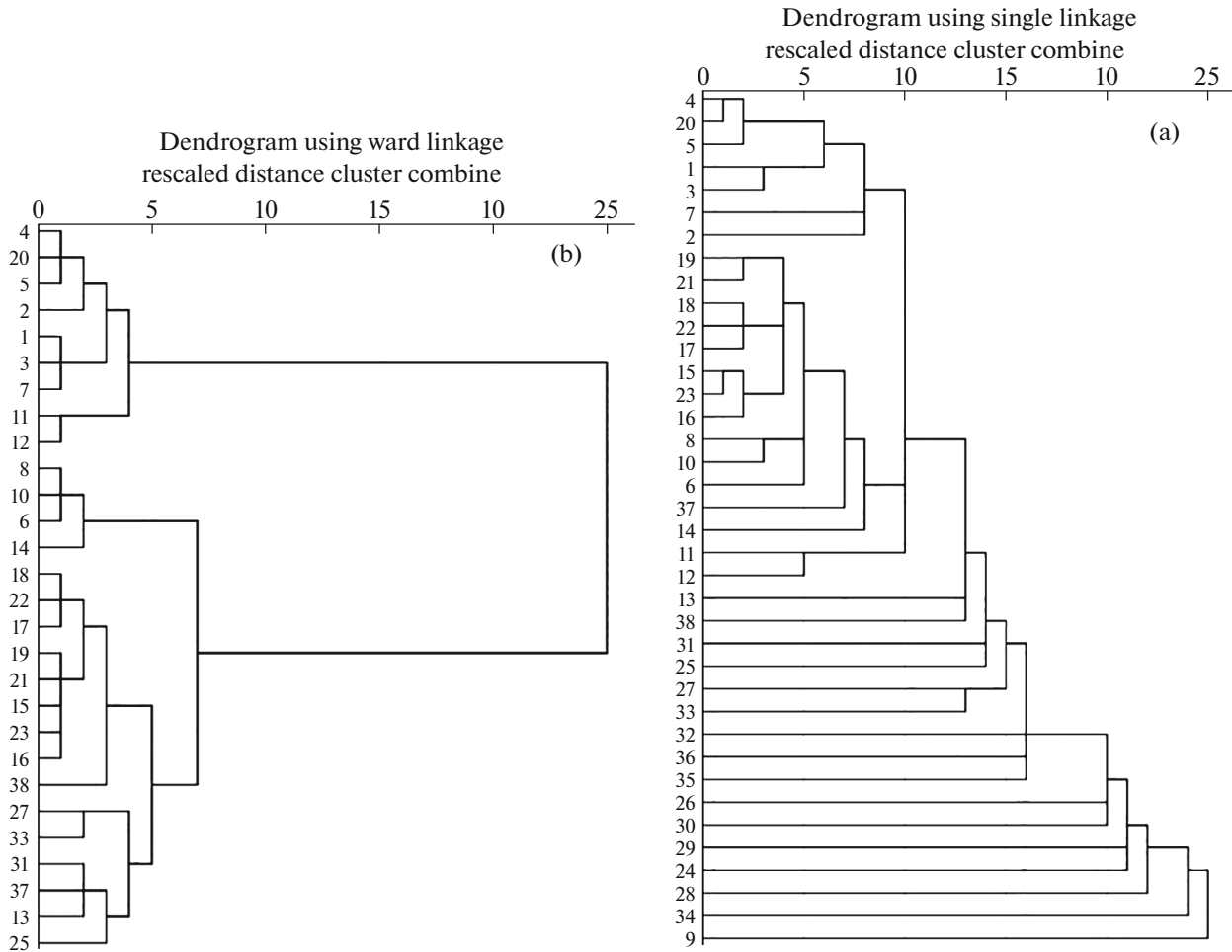


**Fig. 6.** Dendrogram resulting from cluster analysis for all studied stations: (a) before eliminating stations with low correlations, (b) after eliminating stations with low correlations.

tion (mCd) values for the studied samples indicated that the studied samples are devoid of significant ecological risk (Table 11). It is worth mentioning that agricultural activities in this region could potentially elevate this risk in the future. In addition to the employed indices for determining pollution and assessing the hazardous nature of the study area, two additional indices, namely Pollution Load Index (PLI) and Potential Ecological Risk (PER), were used to gauge the pollution level of the area. According to these two indices, the studied samples exhibit no considerable pollution (Table 11).

The summary of results obtained from various environmental indices indicates that the studied samples exhibit contamination for elements Mg, Sr, Cr, Ni, Pr, and Cd based on the four indices Igeo, EF, CF, and NIPI. Among these elements, the two heavy metals, Cadmium (Cd) and Strontium (Sr), show the highest levels of contamination according to these indices. Studies related to the soil quality of the plain demonstrate that the concentration of strontium significantly increases in areas with gypsum and saline

units (Gachsaran Formation). Therefore, it is inferred that the origin of this heavy metal could be both natural and due to transported alluvium from the Gachsaran Formation towards the plain areas. Among the

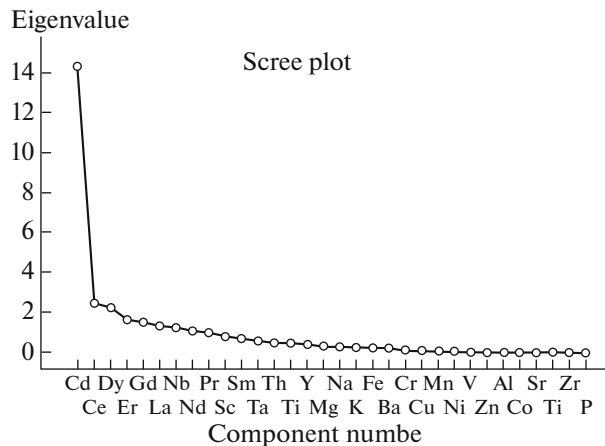


**Fig. 7.** Scree diagram of the studied samples.

**Table 9.** Factor loadings of the studied variables

	Initial eigenvalues							Rounded values						
	factors							factors						
	1	2	3	4	0	6	7	1	2	3	4	0	6	7
Al	5/71	5/33	-5/17	-5/54	-5/33	5/20	-5/27	5/72	5/52	-5/53	5/50	5/55	-5/05	5/10
Fe	5/70	-5/21	-5/53	-5/57	5/52	5/51	5/46	5/73	-5/14	5/15	-5/53	5/54	5/34	5/33
Na	5/25	5/04	5/03	-5/50	5/33	5/17	-5/52	<b>5/27</b>	<b>5/46</b>	-5/12	-5/57	5/11	-5/52	5/11
K	5/70	5/30	-5/55	5/24	5/16	-5/33	5/50	5/76	5/10	5/56	-5/43	5/25	5/51	-5/22
Mg	5/62	5/10	5/04	-5/12	-5/21	-5/51	-5/16	5/04	<b>5/46</b>	5/34	5/13	-5/21	-5/13	5/13
Ti	5/44	-5/15	5/55	5/17	5/20	-5/51	5/55	5/47	5/54	5/53	5/55	5/21	5/21	-5/14
Mn	5/42	5/30	-5/17	-5/12	-5/16	-5/53	5/55	5/44	5/52	-5/53	-5/24	5/55	-5/23	5/25
Ba	5/04	-5/57	-5/44	-5/50	-5/14	5/53	-5/51	5/06	-5/41	-5/54	-5/53	5/55	-5/17	5/50
Zr	5/73	-5/24	5/21	5/12	-5/20	-5/45	-5/54	5/65	-5/57	<b>5/07</b>	-5/51	-5/16	5/55	-5/17
V	5/61	-5/54	5/35	5/07	-5/27	-5/56	5/24	5/02	5/54	<b>5/67</b>	-5/51	<b>5/44</b>	5/55	5/54
Cr	5/66	-5/25	5/52	-5/20	5/32	-5/50	5/27	5/67	-5/56	-5/13	5/54	-5/11	<b>5/02</b>	5/12
Zn	5/06	5/13	-5/43	5/25	-5/14	5/15	-5/53	5/06	-5/24	-5/56	-5/50	5/35	-5/32	5/55
Ce	5/75	5/31	-5/55	-5/23	-5/57	-5/51	5/23	5/72	5/57	-5/55	-5/27	-5/50	-5/57	5/31
Ni	5/52	5/54	-5/50	-5/15	-5/15	5/15	5/11	5/52	-5/51	5/53	5/55	5/53	-5/50	5/24
La	5/72	5/33	-5/54	-5/14	5/53	-5/35	5/11	5/70	5/11	5/55	-5/44	-5/14	5/52	-5/51
Nd	5/70	-5/51	-5/14	-5/54	5/40	-5/54	-5/25	5/75	5/55	-5/35	5/57	5/55	5/10	-5/25
Cu	5/04	-5/20	-5/45	-5/11	-5/56	5/54	5/14	5/06	-5/03	-5/10	-5/51	5/51	5/57	5/13
Y	5/66	5/54	5/25	-5/26	-5/14	5/33	5/24	5/63	5/10	5/50	5/13	-5/52	5/55	<b>5/07</b>
Co	5/76	-5/32	5/56	-5/53	-5/35	-5/54	-5/55	5/73	-5/25	5/37	5/24	-5/14	-5/51	5/50
Sc	5/60	-5/22	5/20	-5/34	-5/52	5/45	5/55	5/63	5/12	-5/52	<b>5/45</b>	-5/10	5/55	5/30
Nb	5/60	-5/47	5/24	5/53	5/24	5/56	5/54	5/62	5/53	5/12	5/45	5/54	5/47	-5/57
Th	5/42	5/11	-5/25	-5/54	5/24	-5/54	-5/50	5/40	5/51	-5/15	-5/11	5/50	5/50	-5/13
Pr	5/20	5/17	-5/50	5/76	5/14	5/34	5/21	<b>5/25</b>	5/55	5/54	5/53	<b>5/52</b>	-5/51	-5/51
Sm	5/42	5/16	-5/57	5/51	-5/50	-5/51	-5/25	5/43	5/54	5/52	5/53	-5/52	-5/27	-5/14
Gd	5/74	-5/50	-5/14	5/57	5/16	5/21	-5/37	5/45	-5/52	-5/17	5/35	5/12	-5/17	-5/24
Dy	5/76	5/26	5/14	5/52	5/14	-5/57	5/55	5/76	<b>5/30</b>	5/53	-5/12	5/57	5/50	-5/53
Er	5/73	-5/57	5/20	5/17	-5/34	-5/13	-5/56	5/65	5/50	<b>5/04</b>	5/56	5/55	-5/55	5/51
Ta	5/67	-5/45	5/55	5/57	5/53	5/25	-5/21	5/64	-5/57	5/15	<b>5/00</b>	5/55	5/56	-5/50
Tl	5/72	-5/36	5/53	5/54	5/10	-5/25	-5/14	5/71	-5/11	5/25	5/10	-5/55	5/26	-5/36

influential factors in soil contamination by other elements, various anthropogenic sources such as agriculture and the utilization of different elements as drilling mud components in multiple wellbore sections being drilled in the upstream section of the studied region can be mentioned.

#### SOURCE IDENTIFICATION OF AREA SEDIMENTS

Source identification of various sediments plays a significant role in determining the origins of multiple pollutants transported to the area through water or wind currents [17]. In these studies, various methods have been employed for precise source identification

of sediments to trace the origins of different pollutants. These methods can serve as templates for similar studies in other parts of the world, which will be further discussed in the following sections.

#### ANALYSIS OF MAIN ELEMENT RESULTS BASED ON THE ALUMINUM SCALE:

The  $\text{SiO}_2/\text{Al}_2\text{O}_3$  ratio serves as a key indicator for determining the origin of sediments and identifying sediment sources [13]. When comparing different oxides with  $\text{Al}_2\text{O}_3$  to identify sediment sources, a positive correlation is observed with  $\text{Fe}_2\text{O}_3$ ,  $\text{K}_2\text{O}$ ,  $\text{MgO}$ ,  $\text{SiO}_2$ , and  $\text{TiO}_2$ , while an inverse relationship is found

**Table 10.** Environmental indicators (Igeo, EF, Cf, NIPI)

Element	Igeo		EF		Cf		NIPI	
	pollution class	percent	enrichment amount	percent	pollution class	percent	amount	level
Al	Completely uncontaminated	100	No to low	100	Low	100	0.45	Low
Fe	Completely uncontaminated	100	No to low	100	Low	100	0.88	Low
Na	Completely uncontaminated	100	No to low	100	<b>Low</b> <b>Medium</b>	<b>94.7</b> <b>5.3</b>	0.19	Low
K	Completely uncontaminated	100	No to low	100	Low	100	0.31	Low
Mg	<b>Completely uncontaminated</b>	<b>73.7</b>	<b>No to low</b>	<b>29</b>	<b>Low</b>	<b>87</b>	<b>1.39</b>	<b>Medium</b>
	<b>Uncontaminated to moderate</b>	<b>26.3</b>	<b>No to low</b> <b>Medium</b>	<b>68</b> <b>3</b>	<b>Medium</b>	<b>13</b>		
Ti	Completely uncontaminated	100	<b>No to low</b> <b>No to low</b>	<b>97.4</b> <b>2.6</b>	Low	100	0.68	Low
P	Completely uncontaminated	100	<b>No to low</b> <b>No to low</b>	<b>100</b> <b>7.9</b>	Low	100	0.79	Low
Mn	Completely uncontaminated	100	<b>No to low</b> <b>Medium</b>	<b>97.4</b> <b>2.6</b>	<b>Low</b> <b>Medium</b>	<b>97.7</b> <b>2.6</b>	0.99	Low
Ba	Completely uncontaminated	100	No to low	100	Low	100	0.62	Low
Sr	<b>Completely uncontaminated</b>	<b>81.6</b>	<b>No to low</b>	<b>27</b>	<b>Low</b>	<b>34</b>	<b>4.09</b>	<b>Medium To Much</b>
	<b>Uncontaminated to moderate</b>	<b>18.4</b>	<b>Medium</b>	<b>47</b>	<b>Medium</b>	<b>50</b>		
	<b>Medium</b>	<b>15.8</b>	<b>Much</b>	<b>26</b>	<b>Much</b>	<b>16</b>		
Zr	Completely uncontaminated	100	No to low	100	Low	100	0.68	Low
V	Completely uncontaminated	100	<b>No to low</b> <b>Medium</b>	<b>96.7</b> <b>5.3</b>	Low	100	0.73	Low
Cr	<b>Completely uncontaminated</b>	<b>84.2</b>	<b>No to low</b>	<b>37</b>	<b>Low</b>	<b>34</b>	<b>1.71</b>	<b>Medium</b>
	<b>Uncontaminated to moderate</b>	<b>15.8</b>	<b>Medium</b>	<b>63</b>	<b>Medium</b>	<b>66</b>		
Zn	Completely uncontaminated	100	<b>No to low</b> <b>No to low</b>	<b>96.7</b> <b>5.3</b>	Low	100	0.78	Low
Ce	Completely uncontaminated	100	No to low	100	Low	100	0.48	Low
Ni	<b>Completely uncontaminated</b>	<b>92.1</b>	<b>No to low</b>	<b>50</b>	<b>Low</b>	<b>45</b>	<b>1.85</b>	<b>Medium</b>
	<b>Uncontaminated to moderate</b>	<b>7.9</b>	<b>Medium</b>	<b>50</b>	<b>Medium</b>	<b>55</b>		
La	Completely uncontaminated	100	No to low	100	Low	100	0.56	Low
Nd	Completely uncontaminated	100	No to low	100	Low	100	0.55	Low

Table 10. (Contd.)

Element	Igeo		EF		Cf		NIPI	
	pollution class	percent	enrichment amount	percent	pollution class	percent	amount	level
Cu	Completely uncontaminated	100	No to low Medium	97.4 2.6	Low	100	0.77	Low
Y	Completely uncontaminated	100	No to low Medium	97.4 2.6	Low	100	0.56	Low
Co	Completely uncontaminated	100	No to low Medium	96.7 5.3	Low	100	0.87	Low
Sc	Completely uncontaminated	100	No to low Medium	97.4 2.6	Low	100	0.60	Low
Nb	Completely uncontaminated	100	No to low Medium	92.3 7.9	Low	100	0.80	Low
Th	Completely uncontaminated	100	No to low	100	Low	100	0.36	Low
Pr	Completely uncontaminated	94.7	No to low	96.7	Low	94.7	1.71	Medium
	Uncontaminated to moderate	5.3	Medium	5.3	Medium	5.3		
Sm	Completely uncontaminated	100	No to low	100	Low	100	0.67	Low
Gd	Completely uncontaminated	100	No to low Medium	97.4 2.6	Low	100 100	0.70	Low
Dy	Completely uncontaminated	100	No to low	100	Low	100	0.62	Low
Er	Completely uncontaminated	100	No to low	97.4	Low	100	0.54	Low
Ta	Completely uncontaminated	100	No to low	100	Low	100	0.70	Low
Tl	Completely uncontaminated	100	No to low	100	Low	100	0.33	Low
Cd	Completely uncontaminated	2.6	No to low	3	Medium	50	4.13	Medium
	Uncontaminated to moderate	50	Medium	47	Much	50		
	Medium	47.4	Much	50				

with CaO (Fig. 8). The positive relationship between SiO<sub>2</sub> and Al<sub>2</sub>O<sub>3</sub> can be attributed to the presence of these elements in quartz. In sedimentary rocks, a SiO<sub>2</sub>/Al<sub>2</sub>O<sub>3</sub> ratio greater than 5 to 6 indicates a high degree of maturity of the sedimentary rock [15]. This positive correlation may indicate the presence of feldspars, mica and clay minerals [17].

Examination of the variations of TiO<sub>2</sub> and Al<sub>2</sub>O<sub>3</sub> shows a positive correlation between these two oxides (Fig. 8). Titanium (Ti) is mainly concentrated in phyllosilicates and serves as a reliable indicator for interpreting the origin of sedimentary

rocks because of its limited mobility and translocation during depositional processes compared to other trace elements [5, 6]. These analyses are of great value for further interpretations related to the origin of sediments.

#### GEOCHEMICAL CLASSIFICATION OF SEDIMENTS:

The classification of arkosic and lithic arenites and consequently determining the primary provenance of the sandstones present in soil samples is carried out

**Table 11.** Environmental indicators (PER, PLI, mCd)

No.	mCd	Sample quality	PLI	Pollution load factor	PER	Biological hazard
1	0.51	Low	0.38	Uncontaminated	17.20	Low
2	0.38	Low	0.28	Uncontaminated	14.31	Low
3	0.54	Low	0.42	Uncontaminated	16.28	Low
4	0.43	Low	0.32	Uncontaminated	11.37	Low
5	0.46	Low	0.32	Uncontaminated	12.42	Low
6	0.79	Low	0.65	Uncontaminated	26.35	Low
7	0.53	Low	0.41	Uncontaminated	14.92	Low
8	0.73	Low	0.61	Uncontaminated	23.62	Low
9	0.94	Low	0.78	Uncontaminated	36.84	Low
10	0.71	Low	0.59	Uncontaminated	22.39	Low
11	0.55	Low	0.35	Uncontaminated	11.99	Low
12	0.47	Low	0.29	Uncontaminated	9.97	Low
13	0.76	Low	0.49	Uncontaminated	15.81	Low
14	0.72	Low	0.57	Uncontaminated	24.30	Low
15	0.60	Low	0.51	Uncontaminated	18.72	Low
16	0.66	Low	0.53	Uncontaminated	20.19	Low
17	0.69	Low	0.56	Uncontaminated	19.78	Low
18	0.74	Low	0.60	Uncontaminated	23.31	Low
19	0.65	Low	0.50	Uncontaminated	16.39	Low
20	0.43	Low	0.32	Uncontaminated	11.27	Low
21	0.62	Low	0.48	Uncontaminated	16.84	Low
22	0.70	Low	0.57	Uncontaminated	21.78	Low
23	0.60	Low	0.51	Uncontaminated	17.79	Low
24	0.59	Low	0.48	Uncontaminated	18.80	Low
25	0.59	Low	0.43	Uncontaminated	15.49	Low
No.	mCd	Sample quality	PLI	Pollution load factor	RI	Biological hazard
26	0.71	Low	0.47	Uncontaminated	18.70	Low
27	0.62	Low	0.48	Uncontaminated	20.21	Low
28	0.68	Low	0.54	Uncontaminated	17.15	Low
29	0.58	Low	0.47	Uncontaminated	19.22	Low
30	0.69	Low	0.52	Uncontaminated	18.75	Low
31	0.62	Low	0.45	Uncontaminated	13.80	Low
32	0.55	Low	0.43	Uncontaminated	17.36	Low
33	0.61	Low	0.47	Uncontaminated	24.79	Low
34	0.63	Low	0.48	Uncontaminated	20.28	Low
35	0.62	Low	0.51	Uncontaminated	18.34	Low
36	0.57	Low	0.46	Uncontaminated	16.97	Low
37	0.64	Low	0.48	Uncontaminated	18.53	Low
38	0.62	Low	0.47	Uncontaminated	18.70	Low

using the log (Na<sub>2</sub>O/K<sub>2</sub>O) versus log (SiO<sub>2</sub>/Al<sub>2</sub>O<sub>3</sub>) diagram, which is based on chemical maturity indices [11]. The plotting of the results of major element analysis onto Fig. 9 revealed that most of the sandstone samples in the study area possess an arkosic composi-

tion. This arkosic composition aligns with the sandstone composition found in the Bakhtiari and Aghajari formations (in the northern part of the region) and could indicate the primary provenance for these sediments.



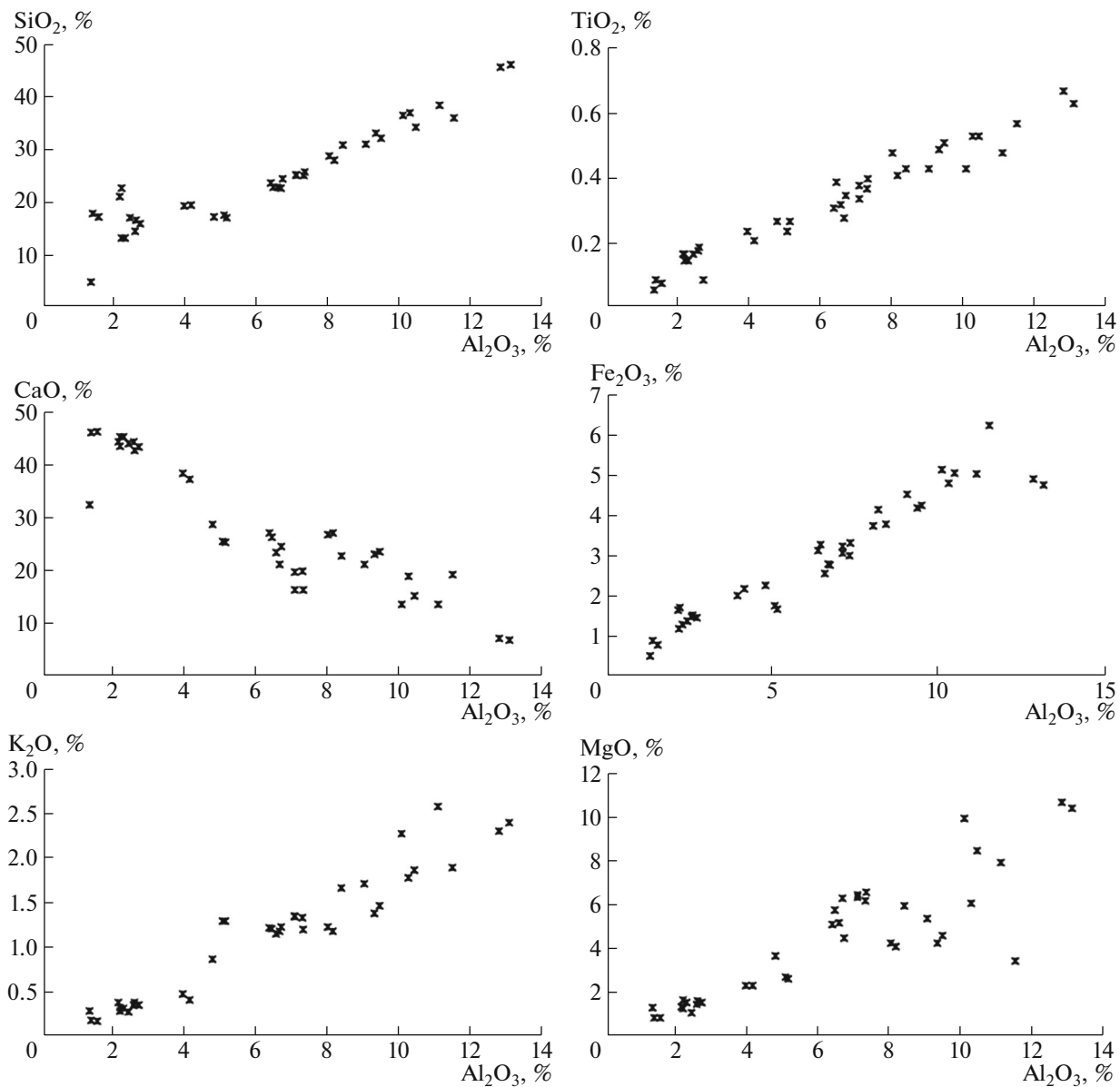


Fig. 8. The trend between aluminum oxide and some of the other studied oxides in the samples.

### PALEOCLIMATIC STUDIES

Plotting SiO<sub>2</sub> against (Al<sub>2</sub>O<sub>3</sub> + K<sub>2</sub>O + Na<sub>2</sub>O) provides insight into the paleoclimatic conditions of the source area and consequently, the determination of the primary origin of the studied sediments [17]. Based on this diagram (Fig. 10), the paleoclimatic conditions of the source area during sediment deposition ranged from humid to semi-arid. This information allows for tracing the primary origin of sediments and the sourceless pollutants in the sedimentary deposits. As previously mentioned, identifying the primary source of sediments plays a crucial role in geochemical analysis for pollution source identification. Given the current warm and dry climate of the study area, these

paleoclimatic conditions suggest that the transported sediments were likely carried by river flows from the upper parts of the watershed known as the "Sannadaj-Sirjan Zone" to the study area.

### SOURCE IDENTIFICATION OF SEDIMENTS USING THE INTEGRATION OF SEDIMENTARY AND GEOCHEMICAL DATA

The composition of sandstones changes during diagenesis and metamorphism [13, 14], so geochemical studies are crucial for identifying the sources of detrital particles and evaluating the degree of pollution in sedimentary rocks [12]. The size of sediment parti-

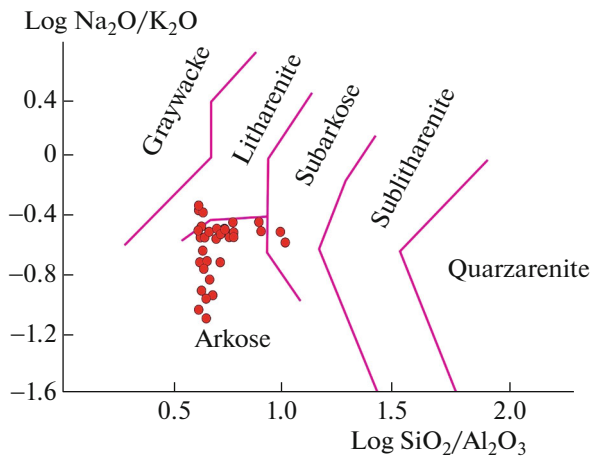


Fig. 9. Geochemical classification of sediments in the study area based on Pettijohn's classification (1987).

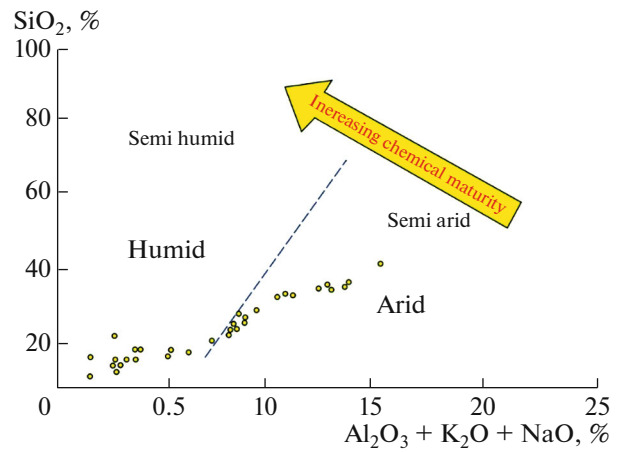


Fig. 10. Diagram depicting the paleoclimatic conditions in the study area according to the chart by Suttner and Dutta (1986).

cles in the region is a major factor affecting dust composition [10]. Sand particles have lower rare earth concentrations than clays [18].

The current source of sand particles in the study area are late Neogene sediments with strong weathering, mainly sandstone and conglomerate types, which are widespread in the Karun River basin [1]. The contribution of the Bakhtiari Conglomerate Formation to fluvial sedimentation is minimal. Clays derived primarily from rock units with high rates of weathering and sedimentation, such as several marl layers in the upstream Gachsaran and Mishan formations, significantly affect the behavior of rare earths in feldspars. Higher enrichment of light rare earth elements indicates an increased clay-to-sand ratio, as clay minerals have a high capacity to adsorb toxic elements [12].

## CONCLUSION

The research conducted has produced numerous results that can be considered a study template for other regions around the world. In the following section, a summary of the results obtained is presented:

—The positive correlation of each element with the source indicator suggests its geologic origin, while the positive correlation with the bioavailability and watershed indicator elements suggests an anthropogenic source for those elements.

—In analysing the dendrogram of the elements, three main clusters can be identified. It seems that elements with geological origin such as Fe are grouped in one cluster, which is probably related to a geological source for these elements. Elements V, Er, Zr, Co, and Mg form one cluster, while elements Mn, Ni, Ce, Y, Al, Sm, K, La, and Dy form another cluster. This could indicate different anthropogenic sources for the mentioned elements.

—Factor analysis showed that seven factors influence the distribution of elements in the studied area, with the most important changes associated with the first factor. According to the factor analysis, all measured elements except Na and Pr are associated with factor 1, which has a high factor loading (above 0.5). Considering the conditions in the region, the presence of various rivers, especially the Karun River, is the probable source of these elements. In the second factor, Na and Mg have the highest factor loading. Evaporite minerals, especially in the eastern part of the region, could be the source of these elements.

—Based on the results obtained from various pollution indices, it can be concluded that the studied samples exhibit moderate contamination for elements including Mg, Sr, Cr, Ni, Pr, and Cd according to the four indices Igeo, EF, Cf, and NIPI. Neglecting environmental factors could contribute to increased soil contamination by these elements in the study area.

—Integration of sedimentological and geochemical data for sediment provenance analysis revealed that the current origin for the sand particles in the studied area is likely Neogene deposits, specifically the Aghajari and Bakhtiari formations, characterized by significant erosion and high sedimentation rates. These deposits predominantly consist of sandstone and conglomerate types and are extensively distributed in the southwestern part of Iran's Karun watershed. However, the contribution of the Bakhtiari Conglomerate Formation to the alluvial sediments transported to the rivers and carried downstream is limited. The probable source for the studied sediments, which are part of rock units with substantial erosion and high sedimentation rates, is likely the numerous marl layers within the Gachsaran and Mishan formations. These formations are situated in the upstream sections of the watershed.

## FUNDING

This work was supported by ongoing institutional funding. No additional grants to carry out or direct this particular research were obtained.

## CONFLICT OF INTEREST

The authors of this work declare that they have no conflicts of interest.

## REFERENCES

1. S. Abbasi, S. Pourmorad, and A. Mohanty, *J. Human Earth, Future* **2** (3) (2021). <https://doi.org/10.28991/HEF-2021-02-03-06>
2. A. Aghanabati, *Geology of Iran* (Geol. Surv. Iran, Tehran, 2004).
3. M. Alavi, *Am. J. Sci.* **311**, 1064–1095 (2007).
4. H. Bagheri Moghadam and N. Kharazian, *Iran. J. Sci. Technol. Trans. Sci.* **44**, 933–953 (2020). <https://doi.org/10.1007/s40995-020-00908-1>
5. A. Heidari and A. Raheb, *J. Sci., India* **17**, 165–179 (2020).
6. L. Komov, A. N. Lukashev, and A. V. Koplus, *Geochemical Methods of Prospecting for Non-Metallic Minerals* (CRC Press, 2021).
7. J. Lee and J. Khim, *Environ. Pollut.* **292** (Pt. A), 118262 (2022).
8. G. D. Love and J. A. Zumberge, *Emerging Patterns in Proterozoic Lipid Biomarker Records (Elements in Geochemical Tracers in Earth System Science)* (Cambridge Univ. Press, 2021).
9. H. Motiei, *Geology of Zagros Oil* (Geol. Org. Iran, 1995).
10. T. V. Oreshkina, G. N. Aleksandrova, and S. M. Lypunov, *Stratigr. Geol. Correl.* **28**, 311–329 (2020).
11. F. J. Pettijohn, *Sedimentary Rocks*, 3rd ed. (Harper & Row, New York, 1987).
12. S. Pourmorad and A. Mohanty, *Alluvial Fans in Southern Iran: Geological, Environmental and Remote Sensing Analysis* (Springer Verlag, Singapore, 2022).
13. S. Pourmorad, R. Harami, A. Solgi, and M. Ale Ali, *Lithol. Miner. Resour.* **56**, 89–112 (2021).
14. H. Rollinson, *Using Geochemical Data (To Understand Geological Processes)* (Univ. Press, Cambridge, 2021).
15. B. P. Roser and R. J. Korsch, *Chem. Geol.* **67**, 119–139 (1996).
16. R. P. Sharma, P. Raja, and B. P. Bhaskar, *J. Geol. Soc. India* **95**, 59–66 (2020).
17. L. J. Suttner and P. J. Dutta, *J. Sediment. Petrol.* **56**, 329–345 (1986).
18. S. R. Taylor and S. M. McLennan, *The Continental Crust: Its Composition and Evolution* (Blackwell, Oxford, 1985).
19. M. Zebari, C. Grutzner, P. Navabpour, and K. Ustaszewski, *Solid Earth* **10** (3), 663–682 (2019).
20. Y. Zhang, *Geochemical Kinetics* (Univ. Press, Princeton, 2021).

**Publisher's Note.** Pleiades Publishing remains neutral with regard to jurisdictional claims in published maps and institutional affiliations.